CHEMISTRY & SUSTAINABILITY
CHEMSUSCHEM
ENERGY & MATERIALS

Accepted Article

Title: Sustainable synthesis of oxalic (and succinic) acid via aerobic oxidation of C6 polyols by using M@CNT/NCNT (M=Fe, V) based catalysts in mild conditions

Authors: Angela Dibenedetto, Maria Ventura, David Williamson, Francesco Lobefaro, Matthew D. Jones, Davide Mattia, Francesco Nocito, and Michele Aresta

To be cited as: *ChemSusChem* 10.1002/cssc.201702347

Link to VoR: http://dx.doi.org/10.1002/cssc.201702347

A Journal of ChemPubSoc Europe

WILEY-VCH www.chemsuschem.org

WILEY-VCH

Sustainable synthesis of oxalic (and succinic) acid *via* aerobic oxidation of C6 polyols by using M@CNT/NCNT (M=Fe, V) based catalysts in mild conditions

Maria Ventura,[a] David Williamson,[c] Francesco Lobefaro,[d] Matthew D. Jones,[e] Davide Mattia,[c]* Francesco Nocito,[b] Michele Aresta,[d] and Angela Dibenedetto[a,b]*

Abstract: Sustainable chemical industry encompasses the shift from fossil carbon to renewable carbon. The synthesis of chemicals from non-edible biomass (cellulosic or oily) represents one of the key steps for “greening” the chemical industry. In this paper we report the aerobic oxidation-cleavage of C6 polyols (5-HMF, glucose, fructose, sucrose) in water to oxalic acid-OA (and succinic acid-SA) under mild conditions using M@CNT/NCNT (M=Fe, V; CNT=carbon nanotubes; NCNT= N-doped CNT), which, under suitable conditions, are recoverable and reusable without any loss of efficiency. The influence of temperature, P_{O2}, reaction time, stirring rate are discussed and the best reaction conditions are emphasized for an almost complete conversion of the starting material, with a good yield of OA equal to 48%. SA and formic acid are the only co-products. The former can be further converted into OA by oxidation in presence of formic acid allowing to reach an overall yield of OA >62%. This process is clean and does not produce organic waste nor gas emissions.

Introduction

The petrochemical industry has contributed to worldwide economic development for the past 150 years or so, but now serious environmental problems are associated with it. The need to establish environmentally friendly chemical processes is an imperative and requires the development of novel and cost-effective methods for pollution prevention.[1] In recent decades, the substitution of non-renewable fossil resources such as crude oil, coal, and natural gas with renewable-carbon such as biomass, including lignocellulose and vegetal oils, as a sustainable feedstock has been extensively investigated for the manufacture of biofuels, commodity chemicals,[2a] high added-value products and new bio-based materials such as bioplastics.[3] Recently, even CO_2 has been taken into serious consideration as building block for chemicals or source of carbon for fuels.[2b] Among renewable feedstock, ligno-cellulosic biomass has attracted considerable attention due to its potential as a source of a wide range of platform chemicals such as C6-polyols,[4] 5-hydroxymethylfurfural (5-HMF),[5] levulinic acid (LA)[6] or formic acid (FA).[7] Among such chemicals, 5-HMF, synthesized by dehydration of fructose, or even directly from glucose,[8] is considered one of the most important intermediates. Its furan structure bearing an aldehyde and a hydroxyl moiety can be transformed into numerous high value chemicals capable of replacing their analogues synthesized from fossil fuels (Scheme 1).

The oxidation-cleavage of glucose (or fructose), has been considered as a candidate for the biomass-based production of monocarboxylic and dicarboxylic acids, a technology that has not yet reached a “sustainable” level today. Recently, efforts have been made to convert C6 into lactic acid,[9] succinic acid or oxalic acid.

Oxalic acid (OA) and its derivatives have widespread application in industrial sectors such as textiles, tanning, oil refining, catalyst preparation, pharmaceuticals, dyes, explosives, straw bleaching, printing, marble polishing, and metal and cloth cleaning.[10] It is also a very important chemical in petroleum refinery, rare-earth and inks manufacturing, rust and corrosion prevention, and dental adhesive processing.[11]

Currently, the methods for producing OA are classified according to the starting raw material into six groups: (i) fusion of sawdust with caustic soda, (ii) oxidation of olefins and glycols, (iii) radiation processing of carbonate solutions and molasses, (iv) fermentation of carbohydrates, (v) oxidation of carbohydrates with nitric and sulphuric acid, and (vi) formates decomposition. The last three are the most used technologies. Fermentation routes to OA have been studied with renewed interest in the last decade, yielding mainly citric acid and/or OA from sucrose or lactose, depending on the fermentation conditions. OA production at the level of >200 mM has been achieved under strict control of pH.[12] The oxidation of C6 with nitric acid is currently the most widely used industrial process to OA. A strong acid solution composed of HNO_3 and H_2SO_4 together with V_2O_5 as the catalyst is used to achieve a conversion of 99% of the substrate with yields of OA from 2.9% to 54%, producing large volumes of waste.[13] Coupling of formates is an attractive route[11,14] which, nevertheless, still uses strong acids and produces waste with high environmental burden. From an environmental point of view, none of the above routes follows the 12 principles of green chemistry.

---

[a] Prof A. Dibenedetto, Dr M. Ventura
CIRCC, Via Celso Ulpiani, 27, 70126 Bari, Italy
E-mail: angela.dibenedetto@uniba.it
[b] Prof A. Dibenedetto, Dr F. Nocito
Department of Chemistry, University of Bari, Campus Universitario, 70126 Bari, Italy
[c] Prof D. Mattia, Dr D. Williamson
Centre for Advanced Separations Engineering and Department of Chemical Engineering, University of Bath, Claverton Down, Bath BA2 7AY, United Kingdom
E-mail: D.Mattia@bath.ac.uk
[d] Prof. M. Aresta, BSc F. Lobefaro
IC^{2}R, Viale Einaudi 25, 70125 Bari, Italy
[e] Prof. M. D. Jones
Department of Chemistry, University of Bath, Bath BA27AY, UK.

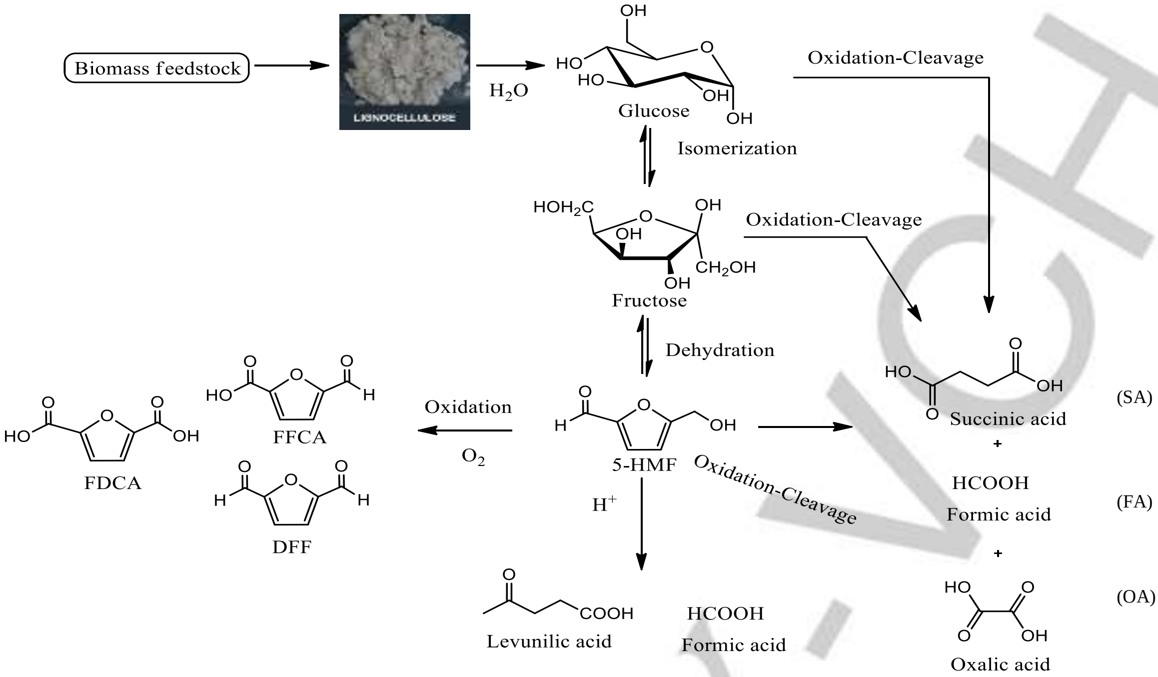

Scheme 1. Representative processes for cellulosic biomass conversion into chemicals

We have recently developed environmentally friendly technologies based on the use of water as solvent and oxygen or even air as oxidant for the conversion of 5-HMF into DFF, FFCA, HMFCA, FDCA,[2,15] targeting high conversion and selectivity. (Scheme 1, left side) Earth abundant metal catalysts in the form of mixed oxides were used with selective oxidation of the ring pending functionalities without touching the integrity of the furan ring. We have now tested in such oxidation metals supported on carbon nanotubes (M@CNT) and have found a completely different behavior with respect to mixed oxides in almost the same operative conditions (*vide infra*). CNTs are a new kind of carbon materials that offer interesting possibilities as support for metal particles, due to the sp^2 carbon structure, the excellent electron transport performance and the electronic interaction of active nanoparticles with the CNTs walls.[16] In the field of biomass transformation, it has been proved that M@CNT are active in a wide range of conversions. It has been reported that Au-Pd nanoparticles deposited on CNTs show higher catalytic activity than on alumina or silica for the base-free aerobic oxidation of 5-HMF towards FDCA.[17] Therefore, CNTs can be considered promising catalyst supports for the selective oxidation of 5-HMF. Accordingly, we present in this paper the use of M@CNTs (M=Fe, V),[18] or M@NCNTs (where NCNT is a nitrogen-doped CNT) in the aerobic oxidation of either 5-HMF, or fructose or glucose or even sucrose in water. We show that the oxidation cleavage of the C6 polyol takes place affording interesting yields of oxalic acid, and succinic acid as co-product. To the best of our knowledge this is the first report on a sustainable synthesis of OA from a C6 polyol with a best potential yield of *ca*. 60%, working under quite mild conditions.

Results and Discussion

Aerobic oxidation of 5-HMF with M@CNT/NCNT

The oxidation of 5-HMF was investigated using the three catalysts, Fe@CNT, Fe@NCNT and V-Fe@CNT in water using O_2 as oxidant. The oxidation of 5-HMF can occur following two alternative routes according to the temperature (Scheme 1): either the furan ring substituents are oxidized (left part) at 383 K, or oxalic acid and succinic acid are formed (right part) at >403 K *via* oxidation-cleavage of the furan ring. No organic solvents were used and the product distribution could be governed by controlling the reaction conditions (*vide infra*), minimizing the waste generated in the process.

An aspect of the reaction that has attracted our attention was the random conversion of 5-HMF into fructose: the reverse of the formation of 5-HMF, never observed in our previous works in which mixed oxides were used as catalysts[2a,15] of oxidation of 5-HMF. The results of the catalytic runs are listed in Table 1, where the activity of Fe@CNT, V-Fe@CNT and Fe@NCNT are compared in different conditions of temperature and stirring rate. The last parameter resulted to be quite important in driving the conversion and selectivity, as we discuss below.

However, according to our habit,[2a,15] after the first catalytic tests, we have recovered the catalyst and verified whether any modification of its structure and/or composition had occurred. The first check we did was on the structure of the catalyst (Entry 1- 2 in Table 1) used at 1000 rpm: leaching of Fe from CNTs was observed by EDX (Energy Dispersive X-ray Spectroscopy) analysis and the breaking of CNTs was detected by TEM (Figure 1a and 1b).

Table 1. Oxidation-cleavage of 5-HMF with Fe@CNT (**A**), Fe@NCNT (**B**) and V,Fe@CNT (**C**) as catalysts

	Cat	rpm	Time (h)	T (K)	Conv. (%)	η% DFF	FFCA	FDCA	FA	OA	SA	Fructose
1	A	1000	3	383	23.7	4.41	89.6	0	5.6	0	0	0
2	A	1000	**3**	403	**99**	0.39	18.8	22.2	8.5	22.0	8.6	29.0
3	A	500	**3**	403	**99**	4.6	2.35	8.0	15.3	30.6	16.3	21.3
4	A	250	**3**	403	**99**	3.2	4.8	0	18.5	**37.8**	17.6	17.7
5	A	250	**1.5**	413	**99**	0	0	0	19.4	**48.4**	7.8	9.2
6	B	250	1.5	413	47.8	11.7	0	0	16.5	**39.8**	10.0	21.8
7	B	250	3	413	90.2	4.9	0	0	27.0	**39.9**	16.2	4.1
8	C	250	1.5	413	62.1	3.3	61.8	0	10.8	19.9	1.4	0
9	C	250	**3**	413	**99**	0	65.1	0	25.1	6.3	3.5	0
10	C	250	**6**	413	**99**	0	<1	0	85.3	14.0	0	0

Reaction Conditions: [5-HMF]= 0.16 M, 0.025 g of catalyst; Acronyms are reported in Scheme 1 and in the text.

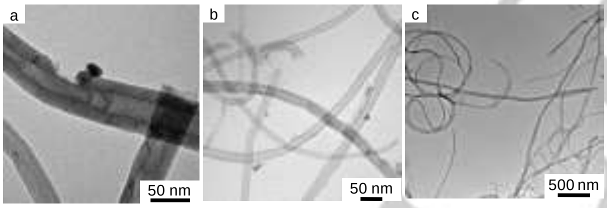

Figure 1. TEM micrographs of catalyst "A" after a run (Fig. 1a and 1b, Entry 1 and 2, Table 1 at 1000 rpm), indicating tube degradation after reaction, with metal nanoparticles partially removed from the tube wall and the tube walls themselves snapped or deteriorated; TEM of "A" after a catalytic run at 250 rpm (Entries 4 and 5) shows little visible damage to the CNT structure (Fig. 1c).

Raman spectroscopy also confirmed the deterioration of the catalyst at 1000 rpm (Figure 2). The D peak at *ca.* 1367 cm^{-1} is commonly attributed to defects or disorder in the carbon nanotube lattice that may occur through damage to the tube structure or incorporation of dopants that do not fit into the lattice as perfectly as sp^2 hybridized carbon, such as nitrogen in Fe@NCNTs, which causes an increase in D peak intensity due to the formation of lattice vacancies. The G peak at *ca.*1581 cm^{-1} is often attributed to graphitic structure and order in a carbon nanotube sample, while the G' peak at *ca.* 2693 cm^{-1} is an indication of long-range order. Thus, the ratio of the D and G peaks (I_D/I_G) can be used as an indication of the overall order and integrity of a carbon nanotube sample. Here, the increase in the I_D/I_G ratio observed (Table 2) indicates that damage occurs to the CNT structure during reaction. An increase of temperature at 1000 rpm (compare Entry 1 and 2 in Table 1) results in a further deeper damage to the CNT structure.

As such, we have reduced the stirring speed and modified the geometry of the stirring bar (from a linear bar to a round bottom magnet with a topping star for better mixing at lower speed) to improve the stability of the catalyst (using a bar at 250 rpm still causes damage to the catalyst).

When the rpm was decreased from 1000 to 500 with the new stirrer, the selectivity towards OA increased to 30.6 %, Entry 3.

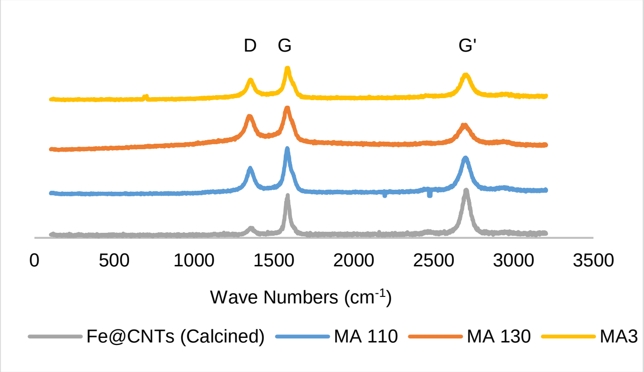

Figure 2. Raman spectra of Fe@CNT catalysts pre- and post-reaction under varying conditions. The X-axis unit is cm^{-1}. MA110=Entry 1; MA130= Entry 2; MA3= Entry 3, 4, Table 1.

Decreasing even more the rpm, the selectivity towards OA further increased to 37.8-48.4%, while the stability of the catalyst increased as shown by TEM (Fig. 1c) and EDX (no leaching of Fe). Therefore, the stirring speed and stirrer geometry influence the stability of the catalyst and, consequently, the selectivity of the process. As a matter of fact at 250 rpm the catalysts was not deteriorated and could be recovered and recycled several times without reducing the conversion and selectivity (See Experimental Section, Catalytic tests).

To investigate the role of the temperature with 250 rpm as optimal rotational speed, an experiment was performed at 413 K, Entry 5, Table 1. The selectivity towards OA increased from 37.8% to 48.4 % while the selectivity towards FA remained almost constant (18.5% vs 19.4%). Further increasing the temperature above 413 K (data not shown) strongly decreases the OA in favor of FA. We then compared the activity of Fe@CNT to that of Fe@NCNT (Entries 6 and 7) and V-Fe@CNT (Entries 8-10), Table 1. Comparing Fe@CNT (Entry 5) with Fe@NCNT (Entry 6), one can see that there is a decrease by 9 points in the selectivity towards OA in the same reaction conditions, but the global conversion of 5-HMF is much lower when Fe@NCNT is used. This can be a consequence of the increased value of the ratio strong acid sites/strong basic sites, n_a/n_b, from 3.6 for Fe@CNT to 4.6 for Fe@NCNT. Noteworthy, in Entries 2-6 a significant rehydration of 5-HMF to fructose is observed. Considerably, in the best operative conditions (413 K, 250 rpm, 1.5 h) comparison of Entries 5 and 6 in Table 1 shows that modifying the nature of the support (from CNT to NCNT) keeping constant the catalyst (Fe), the selectivity towards OA is lowered by 9 points, while the conversion is halved. Conversely, changing the catalyst from Fe (Entry 5) to V-Fe (Entry 8) the product distribution is strongly influenced. FFCA is formed at short reaction times (1.5 h), while FA becomes the prevalent product for long reaction times (Entries 8-10).

It is clear the influence of V in reducing the formation of C4 and C2 species. Noteworthy, V_2O_5 is the catalyst used in HNO_3-H_2SO_4 in processes on stream.

On the other hand, when 20 bar were used the conversion increased with a slight decrease of selectivity towards OA and increase of FA, Entry 3 (C6 species such as FDCA and fructose were also present).

Table 2. The calculated ratios of the D and G peaks of Raman spectra detailed in Figure 2. An increase in I_D/I_G indicates increased disorder in the sample, caused by defects or damage in the CNT support structure

Sample	I_D/I_G
Fe@CNT Calcined	0.19
Entry 1	0.59
Entry 2	0.82
Entry 3-4	0.65

The effect of the oxygen pressure was also investigated, and the results are shown in Table 3. Noteworthy, either increasing the pressure from 10 to 20 bar or decreasing it to 5 bar has a negative effect on the selectivity of OA, which anyway was decreased. The lower pressure caused incomplete cleavage, and decrease of the OA selectivity Entry 1 - Table 3 (fructose was also present in the reaction mixture and other C6 species).

Table 3. Oxidative-cleavage of 5-HMF with Fe@CNT at different oxygen pressures

					Selectivity (%)				
	Rpm	Time (h)	PO_2 Bar	Conv. (%)	DFF	FFCA	FA	LA	**OA**
1	250	6	5	65.2	0	0	41.7	5.3	**25.1**
2	250	1.5	10	91	8.0	4.1	19.8	4.1	**38.4**
3	250	1.5	20	99	1.6	0	40.6	0	**35.9**

Reaction conditions: [5-HMF]I = 0.16 M; 0.025 g of catalyst; T = 403 K.

The optimal pressure is thus 10 bar that minimizes the formation of FA (Entry 2). Most likely at such pressure the optimal $[O_2]$ is built-up in solution, for a controlled oxidation cleavage to 3 C_2. We have carried out a study to gather information on the sequence of formation of the products trying to propose a plausible reaction pathway and understand whether OA is originated from SA and then degrades to FA as the reaction time increases. The study was performed using Fe@CNT at two temperatures: 403 K, and 413 K. It is worth noting that the conversion of 5-HMF was almost quantitative in both reactions. However, the selectivity towards OA reaches its maximum value within 3 h of reaction at 403 K and 1.5 h at 413 K. For longer times (>6 h), OA degrades to FA that increases up to ca. 30%. Obviously, the conversion of 5-HMF is lower at shorter reaction times: from 99% after 3 h to 9.5 % after 30 min. V, Fe@CNT is less active than Fe@CNT (Entries 5, 6 Table 1) at 413 K, 1.5 h. For longer reaction time an increase of FA is observed (Entry 7). In conclusion, the best conditions for

10.1002/cssc.201702347

maximizing the conversion of 5-HMF and the formation of OA are 1.5-3 h at 413 or 403 K. In both cases we have not found a clear evidence that OA is derived from SA.

When V-Fe@CNT was used, significant changes in the product distribution were observed: after 3h, (Entry 9, Table 1) FFCA was the major product of the reaction. When the reaction was performed for longer reaction times, 6 h Entry 10, FA was obtained as the major product (85.3%), making such reaction an interesting route to FA from C6 polyols. Vanadium increases the oxidation power of the catalyst, producing a reduction of the oxidation temperature (Fig. 3e, Experimental Section). Therefore, the oxidation-cleavage is easier and FA, that is the pre-ultimate product in the oxidative-cleavage chain of the C6 unit that terminates with CO_2 formation, is predominantly obtained.

Aerobic oxidation of fructose and the role of SA

Two aspects of the results reported above attracted our attention: the hydration of 5-HMF to fructose and the presence of succinic acid. However, we decided to: i) use fructose as substrate instead of 5-HMF and ii) check even in this case whether succinic acid can be converted into OA and there is a stepwise cleavage of the starting C6-skeleton to C4 (SA) + C2 (OA) and further to C1 (FA) compounds. We have, thus, reacted SA with O_2 with and without FA and checked the formation of OA. Table 4 shows the results when fructose or SA was used as substrate. The reactions were performed using Fe@CNT as catalyst. In the reaction performed with fructose at 413 K, in 1 h (Entry 1, Table 4) a low conversion (1.2%) was reached and a mixture of SA+FA was obtained.

After 6h, the overall conversion of fructose was increased to 30.5%, OA being the major product and SA present at similar concentration than FA (Entry 2, Table 4).

For longer reaction times, (12 h, Entry 3, Table 4) fructose was completely converted and FA+OA were the major products. Working at 413 K for 12 h with V-Fe @CNT, a complete conversion was observed with a 22.1% selectivity towards OA (Entry 4) and high formation of FA.

Using SA as starting material, OA is formed very selectively, but the conversion of SA remains around a few percent even if the reaction is left going for a long time (Entries 5-6). Conversely, if FA is added to SA (1:5 w/w), Entry 7, SA is converted into OA at a higher rate. This suggests that FA somehow assists the cleavage of SA into OA. For longer reaction times than 12 h, OA was degraded affording FA.

Table 4. Aerobic oxidation-cleavage reaction of fructose or SA with Fe@CNT (R = residual starting reagents).

							Selectivity (%)		
	Cat	Time (h)	T (K)	Substrate	PO_2 Bar	Conv. (%)	FA	OA	SA
1	Fe@CNT	1	413	Fruct	10	1.2	21.8	-	79.3
2	Fe@CNT	6	413	Fruct	10	30.5	27.3	46.5	26.3
3	Fe@CNT	12	413	Fruct	10	99	31	46. 8	21
4	Fe-V@CNT	12	413	Fruct	10	98	78.6	22.1	0
5	Fe@CNT	6	413	SA	10	2.4	0	98	R
6	Fe@CNT	12	413	SA	10	2.5	0	98	R
7	Fe@CNT	12	413	SA+FA	10	12.5	R	99	R

Table 5. Aerobic oxidation-cleavage reaction of glucose as substrate with Fe@CNT/NCNT

							Selectivity (%)				
	Catalyst	Time (h)	T (K)	PO_2 bar	[Glucose]	Conv (%)	FFCA	FA	OA	SA	Fructose
1	Fe@CNT	24	403	20	0.2	0	-	-	-	-	-
2	Fe@NCNT	6	403	20	0.2	10.3	0	32.9	19.4	24.2	8.4
3	Fe@NCNT	12	403	20	0.2	22.0	0	41.7	27.0	28.3	0
4	Fe@NCNT	6	423	20	0.2	41.8	0	16.4	**37.1**	17.3	29.2
5	V-Fe@CNT	12	403	20	0.2	36.8	12.9	50.1	16.6	17.7	0
6	V-Fe@CNT	12	423	20	0.2	96.6	11.7	31.8	**47.9**	8.01	0

10.1002/cssc.201702347

Aerobic oxidation of glucose (and sucrose) in water

As fructose is usually produced by base-catalyzed isomerization of glucose, the catalysts M@CNT/NCNT were also tested using glucose as substrate. Table 5 shows the results when the reaction was carried out at 403-423 K. A higher temperature was used with respect to 5-HMF and fructose, as preliminary tests did show that at 403 and 413 K the reaction rate was quite low. When Fe@CNT was used as catalyst, Entry 1, no reaction was observed even for long reaction times at 403 K.

However, when Fe@NCNT was used as catalyst at the same temperature (Entry 2, Table 5) glucose was converted (10.3%) into a mixture composed by OA, FA and SA with selectivity of 32.9, 19.4 and 24.2%, respectively. This shows that the support plays a role in the reaction. For longer reaction times (Entry 3, Table 5) the conversion was increased from 10.3 to 22 %, as increased was the amount of FA, OA and SA. At 423 K, after 6 h (Entry 4, Table 5), the conversion increased compared to Entry 2 along with the selectivity towards OA. Using V-Fe@CNT, Entries 5-6, after 12 h the conversion of glucose and the yield of OA increased with the temperature, but significant amounts of FA and other compounds were formed. Moreover, fructose, the product of isomerization of glucose, is also randomly present in the reactions. It is mainly formed when Fe@NCNT is used. Interestingly, at 423 K after 12 h using V-Fe@CNT a significant conversion of glucose was observed (96.6%) with an interesting selectivity towards OA equal to 47.9%. It is worth noting that V-Fe@CNT is more basic than Fe@NCT (Table 6, Entries 1 and 3, column 6). This can favor the conversion of glucose into fructose, more reactive than glucose.

The above data show that glucose is (directly or indirectly) catalytically converted into OA with *ca.* 97% conversion and 48% selectivity, under much milder conditions than using technologies today on stream and with a zero air-emission and a reduced formation of waste. We have also used sucrose as starting material, and yields and selectivity were intermediate between fructose and glucose. Moving from 5-HMF to glucose, the rate of oxidation increases in the order: glucose<fructose<5-HMF. In any case an almost quantitative conversion of the substrate was observed with a selectivity around 48%, but in different temperature conditions and using different catalysts.

Conclusions

M@CNT/NCNT catalyzes the aerobic oxidation of C6 polyols (5-HMF, fructose, glucose, and even the dimeric sucrose) with O_2 in water at moderate temperature (403-423 K). Although we started using 5-HMF, being this study a continuation of previous investigation on the selective oxidation of side chains of 5-HMF, we moved to fructose from which 5-HMF originates. In the most favorable conditions (413 K, 1.5 h and 10 atm of O_2), using Fe@CNT, a conversion of 5-HMF equal to 99% was observed with 48.4 % yield of OA and 7.8 % SA. Starting from fructose a conversion equal to 99 % was observed after 12 h, with 46.8 % selectivity towards OA using Fe@CNT at 413 K (Entry 3, Table 4), while V-Fe@CNT produces mainly FA (Entry 4, Table 4). Glucose requires higher temperature: at 423 K the conversion was 96.6 % with a selectivity towards OA equal to 47.9 %, using V-Fe@CNT. The data shown above indicate that different substrates demand different catalysts and reaction conditions. 5-HMF is the easiest substrate for producing OA, glucose the most hard to convert. As a matter of fact, as Scheme 1 shows, glucose must be first isomerized to fructose (basic catalysis) which is then dehydrated to 5-HMF (acid catalysis), the best source of OA. As shown in Table 6 Fe@CNT, V-Fe@CNT and Fe@NCNT have different strong n_a/n_b indexes, Fe@NCNT being the most acid and V-Fe@NCNT the most basic. It is not surprising, thus, that V-Fe@CNT is the most effective catalyst for glucose oxidation to OA, most likely because is the one that facilitates the isomerisation to fructose and further oxidation cleavage.

The conversion of the various substrates and the yield of OA are not too different from the best figures obtained with technologies on stream, but the reaction conditions are much milder and safer, than the harsh conditions used (HNO_3-H_2SO_4-V_2O_5) in processes on stream, with no air born emission and limited waste represented by FA and SA that can be separated.

We have also shown that succinic acid can be converted into oxalic acid in presence of formic acid. However, if SA is converted into OA, a putative total yield of oxalic acid equal to *ca*. 55-60% can be targeted starting from 5-HMF (that can be still optimized) or nearly equal starting from fructose and glucose in the suitable reaction conditions. The catalytic conversion of C6 presented in this paper responds to the criteria of sustainability as it occurs in mild conditions, using recoverable and reusable catalysts, O_2 as oxidant and water as solvent, without generating any air borne emission: further investigation is going on in our laboratory aimed at up-scaling.

Experimental Section

Materials and analytical methods

Oxides for the synthesis of the catalysts, and standard: 2,5-furandicarboxaldehyde ≥99%, 5-formyl-2-furoic acid >99%, 2,5-furandicarboxylic acid >99%, D-glucose, D-fructose, oxalic acid, formic acid, succinic acid and levulinic acid were purchased from Sigma Aldrich. 5-(hydroxymethyl)-furfural was prepared as reported in ref. 5. All the reaction products were analyzed by using a Jasco HPLC equipped with an RI detector and a Phenomenex Rezex RHM Monosaccharide H+(8%) 300x7.8mm at 343 K. A 0.005 N solution of sulphuric acid was used as the mobile phase. The flow rate was between 0.5-0.9 mL/min. The concentration of the substrate and of reaction products were determined using an RI detector.

The surface characterization of the catalysts was carried out by using the Pulse ChemiSorb 2750 Micromeritics instrument. Analyses of the acid/basic sites were carried out using NH_3 or CO_2, respectively, as probe-gas using 100 mg of catalyst. The samples were pretreated under N_2 (30 mL min^{-1}) flow at 673 K. The Pulse Chemisorb was performed with NH_3 or CO_2 gas using He as carrier gas (30 mL min-1).

Brunauer Emmett Teller (BET) surface area was determined using N_2/He as carrier gas at 273 K followed by heating up to 923 K.

Temperature Programmed Desorption (TPD) was performed under He flow at 30 mL min^{-1}. H_2-TPR analysis was carried out using a mixture of H_2/Ar as carrier gas (30 mL min^{-1}) at room temperature, the sample was heated up to 1273.15 K. Elemental analysis was carried out by using EDX (Energy-dispersive X-ray spectroscopy).

Catalysts preparation

Fe@CNTs and Fe@NCNTs were prepared via a floating catalyst CVD method in a quartz tube (25 mm ID, 28 mm OD x 122 cm Length), which was placed into a tube furnace to control the reaction temperature. During the reaction, a precursor solution (45 mL) was loaded into a 50 mL syringe, which was then placed onto a syringe pump for automated injection once the reactor had reached the desired reaction temperature.[18] To synthesize Fe@CNTs, the precursor solution consisted of 1.0 g ferrocene (FcH) dissolved in 50 mL toluene (20 mg/mL). To synthesize Fe@NCNTs, toluene was replaced with acetonitrile in the precursor solution to act as a nitrogen source. During synthesis, the quartz tube was purged with 50 mL Ar as the tube furnace ramped up to the desired reaction temperature of 1063 K at a rate of 5 °/min. When the reaction temperature was reached, the desired precursor solution was injected at a rate of 10 mL/h for 4 hours under a flow of 50 mL H_2 and 400 mL Ar. The quartz tube was then left to cool to room temperature before the fresh catalyst was collected as a black, powdery material. This typically provided a yield of ca. 1.4 g catalyst per synthesis.

To achieve 0.5 wt. % vanadium doping, 0.013 g $VO(acac)_2$ was dissolved in 15 mL methanol. 0.5 g fresh catalyst was then added to this solution to produce a dark slurry, which was stirred in a beaker at room temperature under a hood for 24 hours. After stirring, the methanol had typically evaporated completely and the dry, doped catalyst could be easily collected.

Previous studies have shown that, immediately after synthesis, the iron nanoparticles embedded in the walls of the Fe@CNTs are obscured by a graphitic carbon layer.[18] This prevents them from participating as catalytic sites. To expose these iron particles, the graphitic carbon layer must be removed *via* thermal oxidation in air, without damaging the CNT support structure. This was achieved by packing 0.45 g catalyst into a ¼" x 12.5 cm stainless steel tube, which was loosely packed with quartz wool at the bottom to allow for air flow while preventing the catalyst from escaping. For Fe@CNT based catalysts, the catalyst was heated in a muffle oven at 843 K for 40 minutes, ramping up at a rate of 10 K/min. For Fe@NCNTs, the catalyst was activated at 673 K for 1 hour, due to the decreased stability of the NCNT support structure after nitrogen doping. This thermal activation step was always carried out following the vanadium doping step.

Characterization of the catalysts

Table 6 presents the BET surface area and acid-base properties of the different metal-nanotube catalysts used in the production of OA. The total and strong basic and acid sites were calculated from the area under the peaks in the TPD experiments, and are expressed as the volume of CO_2 and NH_3 up-taken and released, respectively. The ratio strong acid/basic sites (n_a/n_b) is also reported.

A comparison between Entries 1 and 2 in Table 6 reveals that when CNTs were doped with nitrogen (NCNT), a non-equal drop in acid or basic sites was observed resulting in an increase in the ratio na/nb. A different behavior was observed when vanadium was included in the catalysts: a huge increase in both acid and basic sites was observed, but with a resulting lower na/nb ratio. Therefore, both doping CNT with N and adding V as metal, change the properties of the catalyst. Concerning the BET surface area, no major differences were observed for the three catalysts.

The redox behavior was investigated via H_2-TPR analysis.

Table 6. BET surface area and basicity/acidity strength of different Fe@CNT.

Solid	Total CO_2 ads (mL/g)	Strong CO_2 ads (mL/g)	Total NH_3 ads (mL/g)	Strong NH_3 ads (mL/g)	Strong na/nb	BET surface area (m^2/g)
1. Fe@CNT	0.55	0.55	2.25	1.987	3.6	78
2. Fe@NCNT	0.40	0.39	1.94	1.847	4.6	81
3. V-Fe@CNT	1.59	1.46	3.85	3.613	2.5	81

Figure 3a displays the H_2 consumption profile for Fe_2O_3, Fig. 3b that of V_2O_5, Fig. 3c for Fe@CNT, Fig. 3d for Fe@NCNT and Fig. 3e for V-Fe@CNT.

Generally, the reduction of pure Fe_2O_3 to metallic iron can be expressed by the following consecutive transitions: $Fe_2O_3 > Fe_3O_4 > FeO > Fe$[19] that are identified in the profile shown in Fig. 3a, with $\alpha = 370$ °C, $\beta = 619$ °C, $\gamma = 707$ °C.[19,20] (Note: The equipment does not allow to express the temperature as K, therefore we discuss the properties of the catalysts using the Celsius scale of temperature). As displayed in Fig. 3b, H_2-TPR profiles for the sample Fe@CNT show two reductive peaks centered at about 420ºC and 800ºC, respectively.

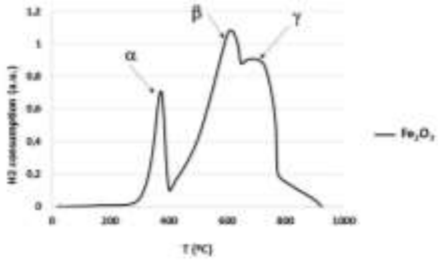

Figure 3a. H_2-TPR profile for Fe_2O_3. α= 370 °C, β= 619 °C, and γ= 707 °C

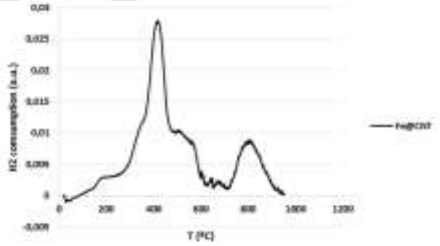

Figure 3b. H_2-TPR profile for Fe@CNT

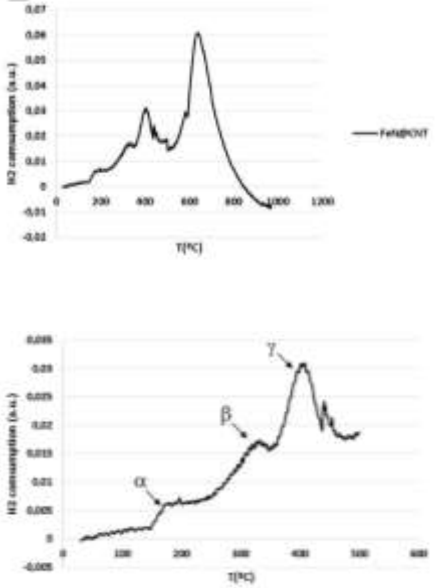

Figure 3c. H_2-TPR profile for Fe@NCNT and its magnified region from 0 to 500 °C

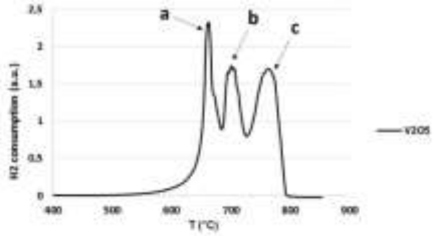

Figure 3d. H_2-TPR profile for V_2O_5

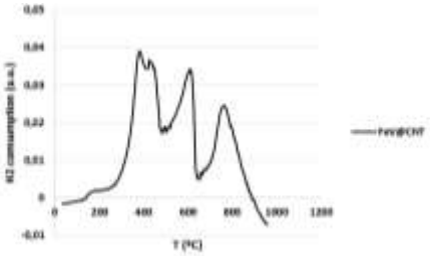

Figure 3e. H_2-TPR profile for V-Fe@CNT

The low temperature peak is likely due to the reduction of Fe^{3+} species to metallic Fe. The high temperature peak can be assigned to the reduction of carbon species on the surfaces of CNTs.[16,21] It can be noted that in the Fe@CNT sample, the three peaks assigned to the three transitions of Fe species, collapse to only one reduction peak. It is possible to identify another reduction peak at low temperature ~185 °C. These facts imply that the confinement of Fe on the CNTs results in an easier reduction. The sample Fe@NCNT shows three peaks in the magnified region at 186, 338 and 400 °C, located at lower temperature than in pure Fe_2O_3. This is an evidence of the different interaction of Fe with NCNTs than with CNTs.

H_2-TPR profile for pure V_2O_5, Fig. 3d, shows three reduction peaks, a = 662 °C, b = 703 °C, c = 764 °C associated to the transitions: $V_2O_5 > V_6O_{13} > V_2O_4 > V_2O_3$.[22] In an attempt to attribute the relevant transitions to Fe or V in V-Fe@CNT (Fig.3e), the peak at lowest reduction temperature centered at 386 °C is tentatively attributed to the transitions belonging to Fe and the other two to the transitions of V. Both values are present at lower temperatures than in pure oxides.

Catalysts characterization by using surface techniques

SEM of the as produced Fe@CNT (Fig. 4a) show the formation of aligned bundles of nanotubes. The micrograph is representative for all catalysts produced. TEM micrographs of the V-Fe@CNT catalyst after activation (Fig. 4b) show the presence of a large number of metal catalyst particles on the surface of the nanotubes without the graphitic coating, making them active for catalysis. The small D and large G and G' peaks observed in Fe@CNTs (Fig. 5) indicate good purity and long-range order in the CNT support structure. Conversely, the increased I_D/I_G ratio and suppressed G' peak observed in Fe@NCNTs indicate the alteration of the sp^2 carbon structure as a result of nitrogen doping. V-Fe@CNTs also show increased disorder compared to the base material, as a result of the vanadium doping process, though a degree of long-range order is maintained.

This is confirmed by the presence of the G' peak at *ca*. 2788 cm^{-1}. The I_D/I_G ratios per each catalyst are reported in Table 7.

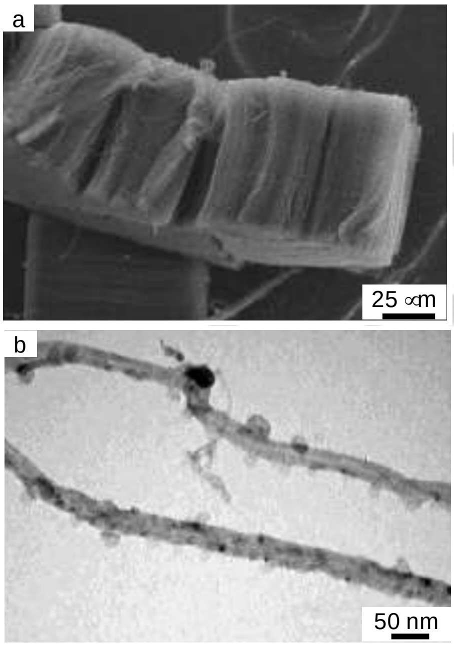

Figure 4. a) SEM micrograph of Fe@CNT; b) TEM micrograph of V-Fe@CNT. Both are representative of other catalysts

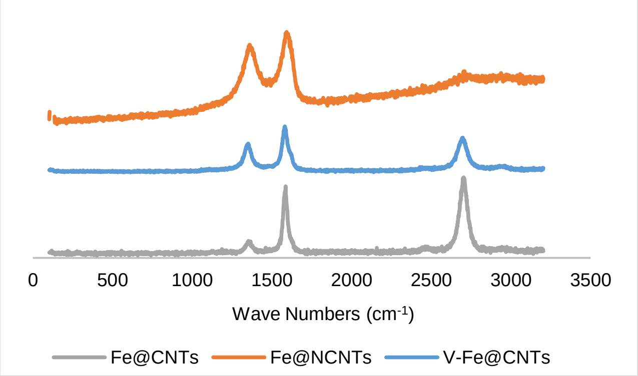

Figure 5. Raman spectra of activated Fe@CNTs, Fe@NCNTs, and V-Fe@CNTs

Table 7. The calculated I_D/I_G ratios of Fe@CNTs, Fe@NCNTs, and V-Fe@CNTs following activation to remove the graphitic carbon layer

Sample	I_D/I_G
Fe@CNTs	0.19
V-Fe@CNTs	0.69
Fe@NCNTs	0.91

XRD analysis (Fig. 6) of Fe@CNTs, Fe@NCNTs, and V-Fe@CNTs was conducted prior to reaction. All materials displayed a strong peak at 26.2°, which is indicative of the CNT support structure. Peaks at 30.4°, 35.8°, 43.2°, 54.3°, 57.8°, and 62.8° all indicate the expected presence of Fe_2O_3 in all samples,[23] though they are less pronounced in the Fe@NCNTs. This is likely due to the lower activation temperature employed to remove the graphitic layer from the catalytic nanoparticles (673 K compared to 843 K), resulting in less complete oxidation of the iron.

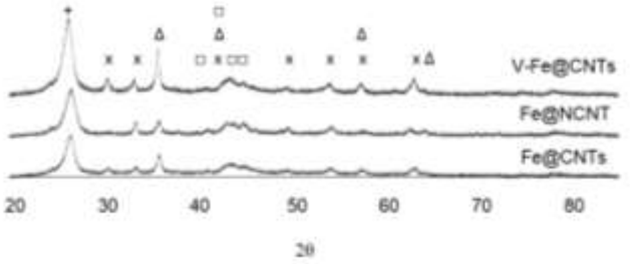

Figure 6. XRD spectra of activated Fe@CNTs, Fe@NCNTs and V-Fe@CNTs. Spectra indicate the presence of the CNT support (+), Fe_2O_3 (x), Fe_3O_4 (Δ) and iron carbide species (□).

Peaks at 35.8°, 43.2°, 57.8°, and 64.0° all indicate the presence of Fe_3O_4 in all samples.[23] Overlapping peaks at 43.2°, 44.0°, and 45.0° with a small shoulder peak at 41.2° indicate the presence of iron carbides such as Fe_3C and Fe_5C_2, with Fe_3C being the most likely to occur.[23] These peaks appear more defined in the Fe@NCNTs once again due to the lower activation temperature used, resulting in less oxidation of the iron, which has been shown elsewhere to exist mostly as metallic iron, iron carbides and iron nitrides prior to activation in air.[18,23] The harsher activation conditions used on Fe@CNT and V-Fe@CNTs thus convert more of the initial carbide phase into the oxide.

Catalytic tests

The conversion of the C6 substrate (5-HMF, fructose, glucose or sucrose) at a fixed temperature was studied in a 50 mL stainless-steel reactor equipped with a withdrawal valve and an electrical heating jacket. 1 mmol of the desired substrate (5-HMF: 0.126 g; D-glucose: 0.180 g, D-fructose: 0.182 g, sucrose 0.340 g; succinic acid: 0.12 g) was dissolved in 5 mL of distilled water in a glass reactor, in which 0.02 g of the catalyst under study and a magnetic stirrer was placed. The glass-reactor was then transferred into the autoclave that was closed and purged three times with O_2. It was charged with the appropriate pressure of oxygen and heated to the reaction temperature as specified in Results and Discussion. At fixed intervals of time, stirring was stopped, a sample of the liquid (0.1 mL) was withdrawn and analysed by HPLC following the disappearance of the substrate. When the concentration of the latter dropped to a constant value (or even zero), the reaction was stopped.

Recycling tests were carried out using Fe@CNT, working at 250 rpm. After a catalytic run (typically Entry 4, Table 1) the catalyst was recovered by centrifugation and reused in four more consecutive runs in the conditions given in Table 1. The conversion remained at 99%, while the selectivity towards OA was 48.0 (run 2), 48.1 (run 3) , 47.9 % (run 4), and 48.0 % (run 5), demonstrating an excellent stability. No Fe was leached.

In all experiments the selectivity toward the i^{th} species is expressed as the ratio of the n_{ith} (mol of the i^{th} species as measured in the reaction mixture) to the $n_{i,t}$ (number of mol of the i^{th} species if the starting material would have been converted 100% into such species). In this way, the sum of selectivities is also the carbon balance, in fact, Σ $s_i = 100$. When the sum is less than 100, it means that there are species that were not quantified. In general, all experiments gave a carbon balance at 99-100%.

Acknowledgements

AD thanks LIDIA Project (CTN01_0063_255060) for partial support. VALBIOR Project (Apulian Region) is gratefully thanked for the use of equipment.

Keywords: oxalic acid from biomass • aerobic oxidation • glucose • 5-HMF • M@CNT/NCNT (M=Fe, V).

[1] R. D. Perlack, L. L. Wright, A. F. Turhollow, R. L. Graham, B. J. Stokes, D. C. Erbach, **2005**, www1.eere.energy.gov/bioenergy/pdfs/final_billionton_vision_report2.pdf.

[2] a) M. Ventura, A. Dibenedetto, M. Aresta, *Inorg Chim Acta*, **2018,** *470*, 11-21; b) M. Aresta, A. Dibenedetto, E. Quaranta, "Reaction Mechanism in Carbon Dioxide Conversion, Springer Verlag, **2016**.

[3] Z. Zhang, K. Deng, *ACS Catalysis* **2015**, *5*, 6529-6544.

[4] Q. Xiang,Y. Y. Lee, R. W. Torget, in *Proceedings of the Twenty-Fifth Symposium on Biotechnology for Fuels and Chemicals* Held May 4–7, 2003, in Breckenridge, CO (Eds.: M. Finkelstein, J. D. McMillan, B. H. Davison, B. Evans), Humana Press, Totowa, NJ, **2004**, pp. 1127-1138.

[5] A. Dibenedetto, M. Aresta, L. di Bitonto, C. Pastore, *ChemSusChem* **2016**, *9*, 118-125.

[6] F. D. Pileidis, M. –M. Titirici, *ChemSusChem* **2016**, *9*, 562-582.

[7] J. Yun, G. D. Yao, F. M. Jin, H. Zhong, A. Kishita, K. Tohji, H. Enomoto, L. Wang, *Aiche Journal* **2016**, *62*, 3657-3663.

[8] a) A. A. Rosatella, S. P. Simeonov, R. F. M. Frade, C. A. M. Afonso, *Green Chem*. **2011**, *13*, 754-793; b) X. L. Tong, Y. Ma, Y. D. Li, *Appl.* Catal. A-Gen. 2010, 385, 1-13; c) A. Dibenedetto, M. Aresta, C. Pastore, L. di Bitonto, A. Angelini, E. Quaranta, RSC Adv. 2015, 5, 26941-26948.

[9] L. Li, F. Shen, R. L. Smith, X. Qi, Green Chemistry 2017, 19, 76-81.

[10] Intratec Solutions Enterprise, Economics of Oxalic acid from sugar, Vol. E251110A0, **2017**.

[11] Encyclopedia of Chemical technology, Wiley: Kirk-Othmer, Vol. 9, **1991**.

[12] a) S. K. Mandal, P. C. Banerjee, *Process Biochem*. **2005**, *40*, 1605–1610; b) H. Strasser, W. Burgstaller, F. Schinner, *FEMS Microbiol Lett* **1994**, *119*, 365–370; c) G. J. G. Ruijter, P. J. I. van de Vondervoort, J. Visser, *Microbiology* **1999**, 2569–2576.

[13] a) W. Guo, H. Jiang, Y. N. Huaxue, *J. CA.* **1997**, *45 (4)*, 240-241; b) L. S. Richmond, Vol. US3720591 A, USA, **1973**; c) E. Yonemitsu, T. Isshiki, T. Suzuki, Y. Yashima, in U.S. Patent, Vol. 3,678,107 (Ed.: U. S. Patent), U.S, **1969**; d) C. L. Mehltretter, C. E. Rist, *J. Agr. Food Chem.* **1953**, *1*, 779-783.

[14] G. M. M.-I. Radulescu, L. Cornos, G. Vapler, Vol. RO106878 B1 30: 4 (Ed.: Rom.), **1993**.

[15] a) M. Aresta, A. Dibenedetto, M. Ventura, Italian patent 102016000014339, Italy, **2017**; b) M. Ventura, M. Aresta, A. Dibenedetto, *ChemSusChem* **2016**, *9*, 1096 – 1100.

[16] X. Guo, J. Guan, B. Li, X. Wang, X. Mu, H. Liu, *Scientific Reports Nature* **2015**, *5*, 16451, doi: 10.1038/srep16451

[17] C. Zhou, W. Deng, X. Wan, Q. Zhang, Y. Yang, Y. Wang, *ChemCatChem* **2015**, *7*, 2853-2863.

[18] O'Byrne, J. P.; Owen, R. E.; Minett, D. R.; Pascu, S. I.; Plucinski, P.; Jones, M. D.; Mattia, D. *Catal. Sci. Technol* **2013**, *3*, 1202-1207.

[19] J. Zielinski, I. Zglinicka, L. Znak, Z. Kaszkur, *Appl. Catal. A: Gen*. **2010**, *381*, 191-196.

[20] W. K. Jozwiak, E. Kaczmarek, T. P. Maniecki, W. Ignaczak, W. Maniukiewicz, *Appl. Catal. A: Gen.* **2007**, *326*, 17-27.

[21] H. E. A. Yang, *J. Mol. Catal. A Chem* **2010**, *323*, 33-39.

[22] M. M. Koranne, J. G. Goodwin, G. Marcelin, *J. Catal.* **1994**, *148*, 369-377.

[23] D. R. Minett, J. P. O'Byrne, S. I. Pascu, P. K. Plucinski, R. E. Owen, M. D. Jones, D. Mattia, *Catal. Sci. Technol.* **2014**, 3351-3358

Entry for the Table of Contents

FULL PAPER

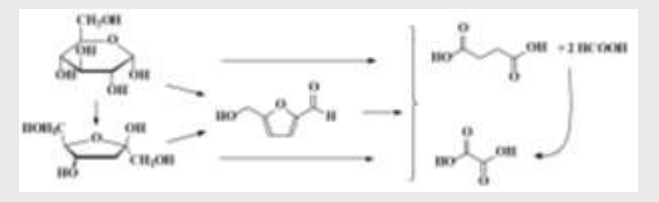

In this paper we report the aerobic oxidation-cleavage of C6 polyols (5-HMF, glucose, fructose, sucrose) in water to oxalic acid-OA (overall yield 48-62%) (and succinic acid-SA) under mild conditions using M@CNT/NCNT (M=Fe, V; CNT=carbon nanotubes; NCNT= N-doped CNT), which are recoverable and reusable without any loss of efficiency.

Maria Ventura,[a] David Williamson,[c] Francesco Lobefaro,[d] Matthew D. Jones,[e] Davide Mattia,[c] Francesco Nocito,[b] Michele Aresta,[d] and Angela Dibenedetto[a,b]**

Page No. – Page No.

Sustainable synthesis of oxalic (and succinic) acid *via* aerobic oxidation of C6 polyols by using M@CNT/NCNT (M=Fe, V) based catalysts in mild conditions